Available at www.sciencedirect.com

ScienceDirect

journal homepage: www.elsevier.com/locate/he

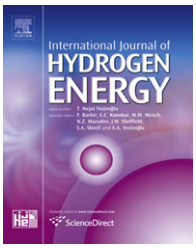

H_2 storage on single- and multi-walled carbon nanotubes

*Gerasimos E. Ioannatos, Xenophon E. Verykios**

Department of Chemical Engineering, University of Patras, GR-26504 Patras, Greece

ARTICLE INFO

Article history:
Received 30 April 2009
Received in revised form
28 September 2009
Accepted 8 November 2009
Available online 22 November 2009

Keywords:
Hydrogen storage
Carbon nanotubes
Adsorption
Temperature
programmed desorption

ABSTRACT

The adsorption of hydrogen on single-walled and multi-walled carbon nanotubes (CNTs) was investigated at 77 and 298 K, in the pressure range of 0–1000 Torr. The adsorption isotherms indicate that adsorption follows the Langmuir model. Hydrogen uptakes were found to depend strongly on the nature of the CNTs. Single-walled CNTs adsorb significantly higher quantities of hydrogen per unit mass of the solid, while the opposite is true on a per unit surface area basis. This observation implies that adsorption takes place selectively on specific sites on the surface. The hydrogen uptake capacity of CNTs was also found to be affected by the purity of the materials, increasing with increasing purity. Temperature programmed desorption indicated that relatively strong adsorption bonds develop between adsorbent and adsorbate and that a single type of adsorption site exists on the solid surface.

1. Introduction

Hydrogen is considered to be the most promising alternative energy carrier in the global energy balance of the future. The use of carbon-based fossil fuels for over a century seems to have caused measurable and catastrophic alterations to the earth's climate. It is widely hoped that the use of carbon-free energy carriers could reverse or decelerate the "greenhouse" phenomenon. However, although hydrogen possesses significant advantages, it also exhibits major drawbacks in its utilization. The most important one being its storage characteristics, which are primarily associated with its use in transportation applications.

There are four major technologies for hydrogen storage: (1) compressed gas, (2) cryogenic liquid, (3) in the form of metal hydrides, and (4) adsorbed on high surface area materials. The first two alternatives are hampered with problems related to tank volume, compression requirements, safety and loss due to evaporation. On the other hand, metal hydrides posses the disadvantages of large weight, excessive cost of manufacture and high temperatures of decomposition.

Adsorption of hydrogen on the surface of porous materials of high surface area could be a viable alternative for hydrogen storage with the potential to meet the capacity goals set by DOE (6.5 wt.%) as well as the advantages of low weight and ease of desorption. Among the materials examined in this respect, carbon nanotubes (CNTs) [1] possess a prominent position.

It has been proposed that hydrogen can be absorbed on carbon nanotubes by physisorption and/or chemisorption. Physisorption occurs when hydrogen maintains its molecular structure and "it is trapped" in the CNTs with Van der Waals forces. In chemisorption, atoms of hydrogen create chemical bonds with the carbon of the nanotubes. Many theoretical studies of the mechanisms of hydrogen adsorption on CNTs have appeared in the literature [2–8]. However, the precise mechanism of hydrogen adsorption on carbon nanotubes is not ascertained. Consequently, it is difficult to determine if

* *Corresponding author*. Tel.: +30 2610 969527; fax: +30 2610 991527.
E-mail address: verykios@chemeng.upatras.gr (X.E. Verykios).
0360-3199/$ – see front matter © 2009 Professor T. Nejat Veziroglu. Published by Elsevier Ltd. All rights reserved.
doi:10.1016/j.ijhydene.2009.11.029

hydrogen is adsorbed exclusively by physisorption or chemisorption also takes place.

Hydrogen can be stored on the inside area of CNTs, shaping a cylindrical monolayer form, or at the outer surface, or between the nanotubes in the case of bundles of carbon nanotubes. Three different places of bonding have been proposed [9]: above the carbon atom (top), in the middle of the C–C bonds (bridge) or in the centre of a hexagonal of carbons (hollow). Moreover, various configurations of hydrogen with respect to its interaction with the walls of the nanotubes are considered, namely perpendicular, longitudinal, and transversal.

Many publications have been devoted to the theoretical study of hydrogen adsorption on CNTs. Monte Carlo simulations [10–12] and other calculations [13–15] have been carried out to predict the hydrogen storage capacity of CNTs, based on the assumption of physical adsorption. The most important factor for these approaches is the choice of the intermolecular potential function that describes the molecular interaction between hydrogen and carbon atoms. Darkrim and Levesque [16], employing a Monte-Carlo numerical simulation in the Grand Canonical Ensemble estimated a maximum storage capacity of CNTs of 11 wt.% at 7.5×10^4 Torr (10 MPa) and 77 K, corresponding to a ratio of hydrogen to carbon atoms of 2.

Experimental studies have reported widely different assessments of hydrogen adsorption capacity of CNTs. Dillon et al. [17], using Temperature Programmed Desorption (TPD), reported that non-purified SWCNTs could store significant amounts of hydrogen, ranging between 5 and 10 wt.%, at room temperature under a pressure of 300 Torr. The TPD experiment suggested that physisorption of hydrogen mainly occurred, as the activation energy of hydrogen desorption was estimated to be 19.6 kJ/mol. Ye et al. [18] measured hydrogen adsorption on purified SWCNTs by a volumetric method, using a Sieverts apparatus, at low temperature (80 K), in the range of 3×10^4–6×10^4 Torr (40–80) bar. The hydrogen storage capacity of those samples was evaluated up to 8 wt.%. Liu et al. [19], using SWCNTs of low purity (50–60%), produced by a semi-continuous hydrogen arc discharge technique and treated with chlorohydric acid, reported a hydrogen storage capacity ranging between 2 and 4 wt.%, at room temperature, under a pressure of 9×10^4 Torr (12 MPa). The high hydrogen uptake is attributed to the presence of cavities or defects which originate from the acid treatment. Similarly, Zhu et al. [20] determined the hydrogen adsorption capacity of MWCNTs (produced by catalytic decomposition of an acetylene-hydrogen mixture at 900 °C) to be up to 5 wt.% at room temperature under the pressure of 7.5×10^4 Torr (100 atm). Finally, Wu et al. [21] measured the hydrogen storage capacity of MWCNTs (obtained by decomposition of CO and CH_4 on powder Co/La_2O_3 catalyst) to be up to 0.25 wt.%, under ambient conditions.

Discrepancies concerning hydrogen storage capacity of CNTs are mainly attributed to: (a) The interaction potential models used to describe the gas-solid interaction, in the case of theoretical analysis. (b) Different experimental conditions employed, primarily temperature. (c) Different production methods of CNTs and consequently different specific surface areas. For example, the CVD method seems to result in CNTs of higher surface areas, as discussed by Basca et al. [22]. (d) Different pre-treatment of CNTs prior to adsorption (heating, vacuum). (e) Different configurations of CNTs, such as tube diameters, tube lengths and inter tube spacing, which permit hydrogen either to move into the tube or to be confined in the interstitial pores. Also, if CNTs are opened in the edge, they are able to adsorb hydrogen on both the inside and outside walls, whereas closed CNTs do not. (f) Different means of purification of CNTs.

Aim of the present study is to provide a better understanding of the parameters which affect surface reactivity and hydrogen storage on CNTs, such as specific surface area and wall thickness, as expressed by single-walled, thin-walled and multi-walled carbon nanotubes, and to investigate desorption characteristics.

2. Experimental

2.1. *Production and characterization of carbon nanotubes*

The CNTs used in the present study were produced by the chemical vapor deposition (CVD) method, employing C_2H_4 (for MWCNTs) or C_2H_2 (for SWCNTs) as carbon source. Mixed oxides of Fe_2O_3 and Al_2O_3 were used as catalytic materials. Further details of preparation of CNTs or catalysts can be found in [23–25].

CNTs were characterized with respect to their crystallinity, wall thickness (single or multi-walled), diameter and length by SEM and Raman spectroscopy. Specific surface area was measured by the BET technique with the use of a Micromeritics (Gemini III 2375) instrument, employing nitrogen physisorption at liquid nitrogen temperatures. Raman analysis was carried out in a Confocal Nikon Modified Raman Microprobe with laser source at 514.5 nm (2.41 eV), readily obtainable from an argon ion laser.

2.2. *Pretreatment of CNTs*

The as-received CNT samples were mixed in 16 M HNO_3 (100 ml per gram of CNTs) for 15 min, under sonication. Subsequently, the samples were washed with distilled water several times until the pH of the rinsing water became neutral, and they were dried overnight at 80 °C. The acid treatment with HNO_3 may remove part of the metal oxide catalyst particles which are incorporated with the CNTs. As the catalyst particles are removed, defects or cavities might be produced on the external surface of CNTs, resulting in increased specific surface area. Acid treatment may also remove other impurities incorporated into the CNTs, such as different forms of carbon.

2.3. *Measurement of hydrogen adsorption isotherms*

A volumetric adsorption apparatus (Fisons, Sorptomatic 1900) was used for the measurements of hydrogen storage capacity of CNTs. The experimental procedure involves the following steps: (a) weighing (200 mg) of pre-treated CNTs and placement of sample in clean sample holder, (b) heating under dynamic vacuum with progressive increase of temperature up

Table 1 – Characteristics of CNTs prepared in the present study by the method of Chemical vapor Deposition (CVD).

	Carbon source	T (°C)	Purity	Specific surface area (m^2/g)	Sp. surface area after HNO_3 treatment (m^2/g)	Diameter	Length	Layers	I_D/I_G ratios
Vulcan XC-72	–	–	–	254	–	–	–	–	–
MWCNTs	C_2H_4	700	95.7%	208	268	10–30 nm	>10 μm	15–35	–
		700	97%	232	275				0.59
		800	99%	243	298				–
thinMWCNTs	C_2H_4	650	95%	309	355	<10 nm	>10 μm	6–10	0.86
SWCNTs	C_2H_2	800	60.5%	726	703	0.8–1.4 nm	>5 μm	1	0.23
			85%	813	877				–

to 250 °C, (c) exposure of the sample to hydrogen (760 Torr) at 250 °C for 1 h, (d) evacuation at 250 °C for 30 min, (e) cooling under vacuum to room temperature, (f) placement of sample in the adsorption apparatus, and (g) evacuation for 15 min and initiation of measurements. Adsorption experiments were conducted at liquid nitrogen temperature (77 K) and at 298 K, in the pressure range between 0 and 1000 Torr.

2.4. *Temperature programmed desorption of H_2*

Temperature-programmed desorption (TPD) experiments were carried out using an apparatus and following the procedures described in detail elsewhere [26]. In a typical experiment, an amount of 100 mg of the sample was placed in a quartz micro reactor, heated at 500 °C under He flow for 15 min and then exposed to flowing hydrogen at 300 °C for 30 min. The sample was heated again at 500 °C under He flow for 15 min, in order to remove adsorbed species from the surface, and then cooled to 25 °C. The flow was then switched to the adsorbing gas, H_2 (40 cc/min) for 1 h, followed by purging with He for 10 min at room temperature (RT). After this step, temperature was increased linearly ($\beta = 30$ °C/min) up to 450 °C and TPD patterns were recorded with the use of a mass spectrometer (Fisons, SXP Elite 300H) connected on-line to the reactor outlet. Responses of the mass spectrometer were calibrated against standard mixtures of accurately known composition.

3. Results and discussion

3.1. *Characterization of CNTs*

The CNTs prepared in the framework of the present study were characterized using SEM, Raman spectroscopy and measurement of total surface area by the BET method. Prior to characterization and use, the CNT samples were pre-treated with HNO_3, following the procedure described earlier. This treatment results in elimination of at least part of the catalyst particles which are encapsulated into the CNTs as well as other materials such as amorphous carbon. As the catalyst particles are removed, defects or cavities are produced on the external surface of CNTs, resulting in increased specific surface area, as reported in Table 1. It should be emphasized that the degree of purity associated and reported with the different CNT samples pertains to purity upon preparation and before acid pre-treatment. Purity was estimated by TGA analysis [23–25].

Fig. 1(A) and (B) show SEM images of SWCNT-85% and MWCNT-99%, respectively. The nanotube structure of the materials is apparent. Differences in tube diameters are also apparent from the SEM image of the multi – walled carbon nanotubes. Raman spectroscopy was employed for the determination of the type of CNT, as well as the presence of defects and amorphous carbon. In the Raman spectra of three materials shown on Fig. 2, a strong band (G-band) at ~1580 $cm^{-1}$is observed, which indicates the existence of

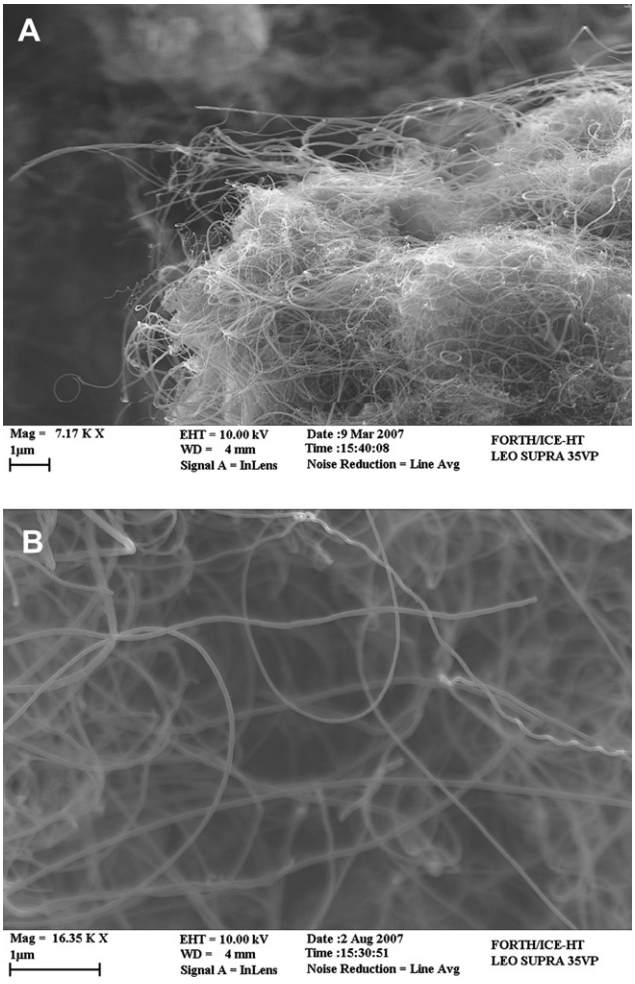

Fig. 1 – SEM image of (A) SWCNTs-85% and (B) MWCNTs-99%.

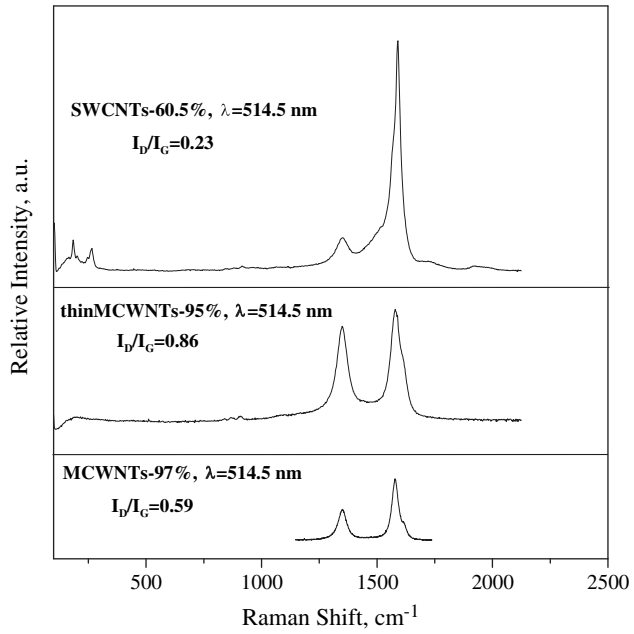

Fig. 2 – Raman spectra of MWCNTs-97%, MWCNTs-95% and SWCNTs-60.5%.

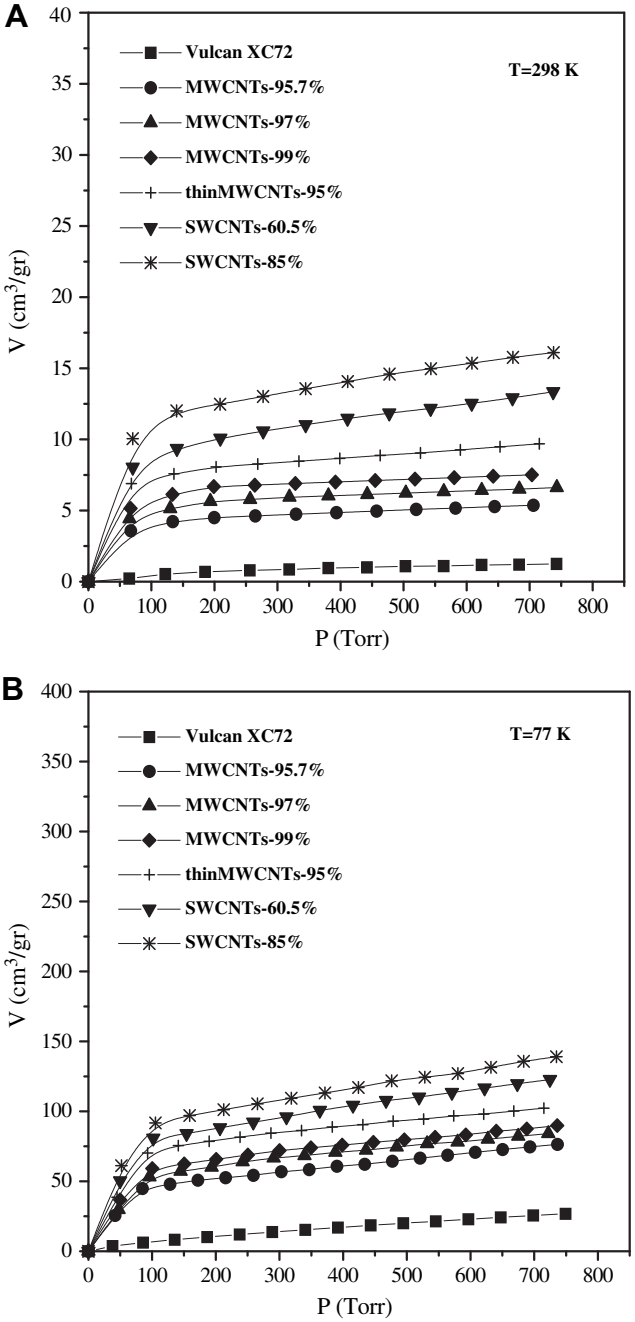

Fig. 3 – Hydrogen adsorption isotherms for different kinds of carbon nanotubes at (A) 298 K, and (B) 77 K.

CNTs and which is attributed to the movements of carbon atoms in opposite directions along the surface of a tube. A weaker peak (D-band) is seen at ~1350 cm^{-1} which originates from defects in the curved graphene sheets and tube ends or in the presence of carbon coating on the outer surface of the tubes. The low values of I_D/I_G ratios, reported in Table 1, clearly indicate that CNTs produced under the present experimental conditions are relatively pure and posses fewer defects. Raman analysis also indicates the existence of RBM (radial breathing vibrational modes) peaks at ~180 cm^{-1} and at ~250 cm^{-1} which correspond to single – walled material of 0.8–1.4 nm diameter (Table 1). The diameter of SWCNTs was estimated using the function: ν (RBM) (cm^{-1}) = 223.75/d (nm).

Table 1 reports various structural characteristics of the materials employed in the present study, as well as the carbon source employed, the temperature of deposition and the purity. It should be pointed out that the specific surface area, as measured by the BET method with nitrogen adsorption at 77 K, of the as prepared materials varies significantly between about 200 m^2/g of the low purity MWCNT material to about 800 m^2/g of the high purity SWCNT material. After acid treatment, the specific surface area of all materials is enhanced, ranging between 268 and 877 m^2/g. This may be due to the fact that removal of impurities creates defects and cavities which enhance total surface area. The length and diameter of the CNTs which are also reported on Table 1 were estimated from analysis of SEM micrographs while the number of layers was estimated by TEM analysis [23–25].

3.2. *Hydrogen adsorption on carbon nanotubes*

Fig. 3 presents hydrogen adsorption isotherms obtained over different kinds of carbon nanotubes at either 298 K (A) or 77 K (B). The materials investigated include MWCNTs of purities of 95.7, 97 and 99%, thin MWCNTs of 95% purity and SWCNTs of 60.5 and 85% purity. Vulcan XC72 is also included in these measurements for comparison purposes and since this is a planar material, in contrast to the other samples which are tubular. Another reason is the fact that Vulcan XC-72 is frequently used as a carrier of platinum for the formation of electrodes in PEM fuel cells. Fig. 3 indicates that hydrogen adsorption on CNTs follows the Langmuir isotherm equation which is based on the assumptions that adsorption cannot proceed beyond monolayer coverage, equivalence of adsorption sites and surface uniformity.

It is observed that all carbon nanotubes adsorb more hydrogen than the planar carbon sheets (Vulcan-XC72), on a per

Table 2 – Hydrogen storage capacities, for different kinds of carbon nanotubes, at room temperature, on a per unit mass or per unit surface area basis.

T = 298 K	H_2 wt.%	H/C	$\frac{cm^3}{m^2}$	V_m (cm^3/g)	V_s (cm^3/g)
Vulcan XC72	0.03	0.0017	0.005	–	–
MWCNTs-95.7%	0.12	0.0071	0.020	4.018	5.370
MWCNTs-97%	0.14	0.0086	0.024	5.213	6.609
MWCNTs-99%	0.17	0.0100	0.025	6.516	7.511
thinMWCNTs-95%	0.22	0.0126	0.027	7.321	9.694
SWCNTs-60.5%	0.30	0.0179	0.017	9.081	13.348
SWCNTs-85%	0.36	0.0220	0.018	11.588	16.105

unit mass of material (Fig. 3) as well as on a per unit area (Table 2 and Fig. 3) basis. At both adsorption temperatures, the hydrogen uptake of Vulcan XC-72 is a linear function of pressure, which can be explained by Henry's law. The main differences between carbon nanotubes and a carbon sheet are the curvature of the graphene sheets and the cavity of the tubes. The available area for adsorption in a CNT is larger than that of an open surface. Furthermore, the potential fields from the opposite walls of the CNTs overlap so that the attractive forces acting on the adsorbate molecules are larger than those of the flat surface.

It is also observed in Fig. 3 that for the same kind of carbon nanotubes, the hydrogen adsorption capacity is increased as the purity of the CNTs is increased. The results observed cannot be attributed only to increased mass of CNTs with increased purity since the differences in purity are small compared to the differences in adsorption capacity. However, upon removal of impurities such as amorphous carbon and metal catalyst, attached to the surface of CNTs, larger outer surface is exposed to hydrogen, improving hydrogen adsorption capacity. Therefore, as the purity of CNTs is increased, the number of available sites for hydrogen adsorption is increased. It must also be emphasized that, as shown in Table 1, the surface area of the materials after HNO_3 treatment increases with increasing purity. Thus, the enhancement of hydrogen adsorption capacity with increasing purity could be directly attributed to this factor. In most probability, not all amorphous carbon or catalyst material is removed with the acid treatment.

Fig. 3 and Table 2 also indicates that single-walled carbon nanotubes (SWCNTs) adsorb larger quantities of hydrogen, on a per unit mass basis, than multi-walled carbon nanotubes (MWCNTs). This may be attributed to a geometric effect, namely that the tubes in the middle of the MWCNTs do not take part in the hydrogen storage process. As a result, the ratio of the number of hydrogen atoms adsorbed per carbon atom in the CNTs, which is reported in Table 2, increases in going from MWCNTs to thin MWCNTs to SWCNTS. Similarly, the hydrogen storage capacity, with respect to mass percent of hydrogen adsorbed, (Table 2), follows identical trend, as expected.

Although the total hydrogen uptake per unit mass of material is higher in SWCNTs than in MWCNTs, the total adsorbed volume of hydrogen (at 760 Torr) per unit surface area of the solid is larger in MWCNTs than in SWCNTs, as shown in Table 2 in the form of cm^3 of H_2 adsorbed at 760 Torr per m^2 of surface area of CNTs. The total surface area of the samples was measured by nitrogen adsorption at liquid nitrogen temperature following the BET equation. These observations imply that the area which is accessible to hydrogen adsorption is not identical to that accessible to nitrogen adsorption and that the mechanism of adsorption of the two molecules is different. For example, in the case of nitrogen, it seems that adsorption may occur in the space between the carbon atoms, in contrast to the case of hydrogen adsorption. An alternative explanation is that hydrogen adsorbs at specific sites, not over the entire available area and, as a result, the coverage of the surface by hydrogen is not complete. Thus, higher surface area does not necessarily imply higher quantity of adsorbed hydrogen. These observations apply to both temperatures of investigation, 298 and 77 K, as shown in Table 2.

The theoretical monolayer adsorption capacity was estimated using Züttel's [3] model for hydrogen adsorption on carbon nanostructures, which assumes that the molecules of hydrogen are spherical and closed-packed. The condensation of a monolayer of hydrogen on SWCNTs-85% with a specific area of 877 $m^2\,g^{-1}$ leads to an adsorption capacity of 1.75 wt.%. This value is significantly larger than the experimentally obtained value of 0.34% (Table 2) at 298 K but significantly lower than the experimental value at 77 K which is 3.27% (Table 3). This observation supports the fact that, at elevated temperature, hydrogen adsorbs on the surface of CNTs on specific sites without covering the entire available area. However, at low temperature (77 K) the adsorption exceeds monolayer coverage. This is reasonable since 298 K is too high a temperature for purely physical adsorption. Chemical adsorption, by creation of chemisorption bonds is structure specific, thus it only takes place at sites which posses specific requirements. The fact that hydrogen adsorption on CNTs is partially chemical at elevated temperature is also supported by the results of the TPD experiments which are discussed below.

Fig. 3B presents hydrogen adsorption isotherms of the different kinds of carbon nanotubes at 77 K. Comparison of the isotherms at 298 K and 77 K indicates qualitative similarities. However, the quantity of adsorbed hydrogen is much higher at 77 K by nearly one order of magnitude, as would be expected since low temperature reinforces the effect of gas-adsorbent attractive interactions. At 77 K the molecules of hydrogen are adsorbed on the outer surface of the nanotube as well as on monolayer of hydrogen that already exists. By calculating the volume of hydrogen adsorbed at monolayer coverage, V_m, using the BET equation, and the maximum volume adsorbed, V_s, at 760 Torr, it can be concluded that V_s is larger than V_m at 77 K, whereas V_s is close to V_m at 298 K, as reported in Tables 2 and 3. Obviously, at 77 K, adsorption can

Table 3 – Hydrogen storage capacities, for different kinds of carbon nanotubes, at 77 K, on a per unit mass or per unit surface area basis.

T = 77 K	H_2 wt.%	H/C	$\frac{cm^3}{m^2}$	V_m (cm^3/g)	V_s (cm^3/g)
Vulcan XC72	0.24	0.0143	0.106	–	–
MWCNTs-95.7%	1.35	0.0811	0.285	41.543	76.378
MWCNTs-97%	1.82	0.1093	0.306	52.107	84.074
MWCNTs-99%	2.00	0.1202	0.301	57.121	89.792
thinMWCNTs-95%	2.29	0.1373	0.288	70.085	102.282
SWCNTs-60.5%	2.74	0.1643	0.157	74.541	122.665
SWCNTs-85%	3.27	0.1960	0.159	85.172	139.036

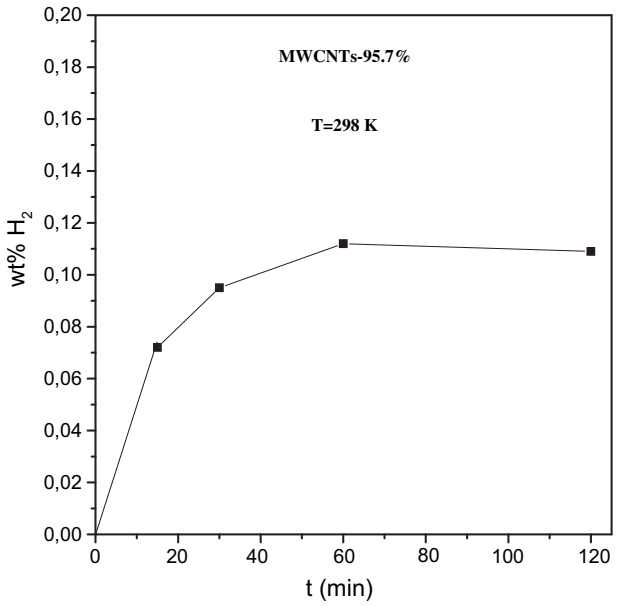

Fig. 4 – Quantity of hydrogen adsorbed under flow conditions at 298 K over the MWCNT-95.7% sample with respect to time of exposure.

proceed beyond monolayer coverage due to the fact that Van der Walls forces become stronger compared to those at 298 K.

All trends which were observed at 298 K and all conclusions concerning the effects of surface area and purity on the quantity of hydrogen adsorbed per unit mass or per unit surface area of the solid are valid in the case of adsorption at 77 K as well.

3.3. *Temperature programmed desorption*

The adsorption – desorption characteristics can also be assessed by Temperature Programmed Desorption which involves adsorption of hydrogen on the CNTs at a specific temperature until equilibrium is achieved, followed by desorption while temperature is increased linearly by a specific rate. The temperature at which desorption is taking place and the shape of the desorption peak can be used to obtain qualitative and quantitative information concerning adsorption/desorption characteristics. In this type of experiments, it is important to ascertain that equilibrium adsorption is achieved under conditions of flow prior to initiation of the desorption procedure. In the present study this was investigated by performing adsorption of hydrogen under flow conditions over variable time and measuring the quantity of hydrogen adsorbed. Indicative results, in the form of quantity of hydrogen adsorbed per unit mass of material, pertaining to the MWCNT-95.7% sample, at times of exposure between 20 and 120 min are shown in Fig. 4. It is apparent that a time of exposure of at least 60 min is required in order to achieve equilibrium adsorption under the conditions of the present study.

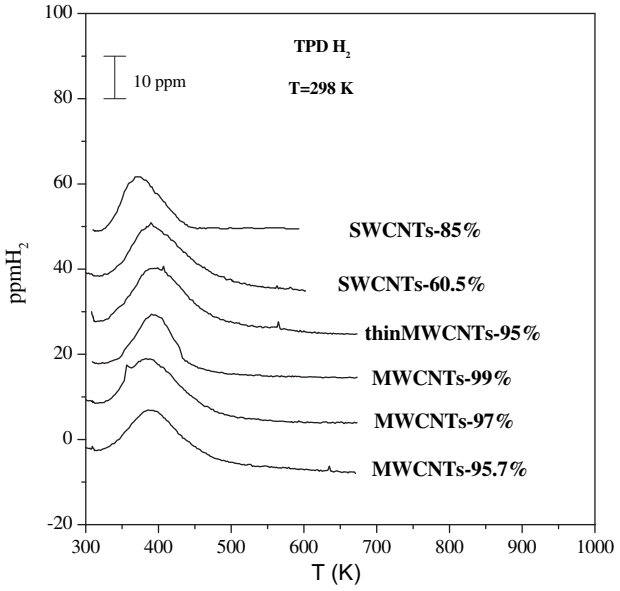

Fig. 5 – Temperature Programmed Desorption spectra of Hydrogen for different kinds of carbon nanotubes.

Table 4 – Hydrogen desorption characteristics, for different kinds of carbon nanotubes, as revealed by TPD experiments.

	H_2%wt. (desorbed)	T_m (K)	E_d (kJ/mol)
MWCNTs-95.7%	0.11	390	20.2
MWCNTs-97%	0.13	392	20.3
MWCNTs-99%	0.16	388	20.0
thinMWCNTs-95%	0.20	383	19.7
SWCNTs-60.5%	0.27	375	19.1
SWCNTs-85%	0.33	371	18.9

Temperature Programmed Desorption (TPD) was used to estimate the quantity of hydrogen desorbed from CNTs upon heating, following adsorption at 298 K. Samples which were exposed to hydrogen at 298 K for more than 60 min were heated up to 450 °C with a heating rate of 30 °C/min. Hydrogen desorption spectra are shown in Fig. 5.

Desorption of hydrogen occurs at temperatures around 373 K, while peak temperature seems to be somewhat affected by the kind of the CNT, as shown in Table 4. Thus, for MWCNTS peak temperature is around 388–342 K, for thin MWCNTs-95% around 383 K and for the SWCNTs around 373 K. It is not surprising that the strength of the adsorption bond, as revealed by the desorption temperature, is influenced by the kind of CNT employed. It is further observed that as hydrogen adsorption capacity increases, the peak of the desorption temperature is moving toward lower temperatures.

The desorption peak maxima can be used to estimate the activation energy of desorption, following equation [17]:

$$\ln\left(\frac{T_m^2}{\beta}\right) = \frac{E_d}{RT_m} \quad (1)$$

where T_m is the temperature at the peak maximum, E_d is the desorption activation energy, β is the heating rate and R is the universal gas constant. The desorption activation energy, which is equivalent to the heat of adsorption in the case of physisorption, is approximately 19 kJ mol^{-1} for the SWCNTs and 20 kJ mol^{-1} for the MWCNTs (Table 4). These values of the desorption activation energy are very close to those reported earlier by Dillon et al. [17], 19.6 kJ/mol. They also support the conclusion derived earlier in this study that hydrogen

adsorption on CNTs is not purely physical in nature but it also involves weak chemisorption bonds.

The quantity of hydrogen desorbed is estimated from the spectra of Fig. 5 by applying a graphical integration method and the results are reported in Table 4. Comparison of the results of hydrogen adsorption at 298 K (Table 2) with the results of the TPD experiments (Table 4) reveals that the quantity of hydrogen desorbed is very close to the quantity of hydrogen adsorbed. This observation reveals that the adsorption sites on the CNTs surface are relatively uniform and that there are no sites which form very weak or very strong adsorption bonds.

4. Summary and conclusions

CNTs of variable wall thickness (multi walled, thin walled and single walled) and of variable purity were prepared by CVD of C2H4 or C2H2 and tested for their hydrogen adsorption capacity at 77 and 298 K, in the pressure range of 0–1000 Torr. The quantity of hydrogen adsorbed at equilibrium was found to be significantly affected by the type of CNT employed or by the wall thickness and by the purity of the CNTs. Maximum adsorption capacity per unit mass of the solid was observed over SWCNTs, followed by thin-walled CNTs and MWCNTs. Adsorption capacity was also observed to increase monotonically with increasing purity. On a per unit surface area basis, hydrogen adsorption capacity was found to follow the opposite trend. These results were discussed with respect to existence of specific adsorption sites on the solid surface. Temperature programmed desorption revealed that there is only a single adsorption site on the surface and that adsorption of hydrogen on CNTs may involve relatively weak chemisorption bonds.

Acknowledgements

This work was funded by the General Secretariat of Research and Technology (GSRT) Hellas and the Commission of the European Community, under the PENED 2003 Program (03ED516) and Dr. Stephanos Nitodas for the Raman spectra.

REFERENCES

[1] Iijima S. Helical mircotubules of graphitic carbon. Nature 1991;354:56–8.
[2] Dresselhaus MS, Williams KA, Eklund PC. Hydrogen adsorption in carbon materials. MRS Bull 1999;24:45–50.
[3] Züttel A, Sudan P, Mauron P, Kyobayashi T, Emenenrgger C, Schlapbach L. Hydrogen storage in carbon nanostructures. Int J Hydrogen Energy 2002;27:203–12.
[4] Lee SM, An KH, Lee YH, Seifert G, Frauenheim T. Novel mechanism of hydrogen storage in carbon nanotubes. J Kor Phys Soc 2001;38:686–91.
[5] Lee SM, An KH, Lee YH, Seifert G, Frauenheim T. A hydrogen storage mechanism in single-walled carbon nanotubes. J Am Chem Soc 2001;123:5059–63.
[6] Lee SM, Lee YH. Hydrogen storage in single-walled carbon nanotubes. Appl Phys Lett 2000;76:2877–9.
[7] Gu C, Gao G-H, Yu Y-X. Density functional study of hydrogen adsorption and separation of hydrogen in single-walled carbon nanotube. Int J Hydrogen Energy 2004;29:465–73.
[8] Rzepka M, Lamp P, de la Casa-Lillo MA. Physisorption of hydrogen 0n microporous carbon and carbon nanotubes. J Phys Chem B 1998;102:10894–8.
[9] Mpourmpakis G, Froudakis GE, Lithoxoos GP, Samios J. Effect of the curvature and chirality for hydrogen storage in single-walled carbon nanotubes: a combined ab initio and Monte Carlo investigation. J Chem Phys 2007;126:144704.
[10] Cheng JR, Yuan XH, Zhao L, Huang DC, Zhao M, Dai L, et al. GCMC simulation of hydrogen physisorption on carbon nanotubes and carbon arrays. Carbon 2004;42:2019–24.
[11] Darkrim FL, Levesque D. Monte Carlo simulations of hydrogen adsorption in single-walled carbon nanotubes. J Chem Phys 1998;109:4981–4.
[12] Marx D, Nielaba P. Path-Integral Monte Carlo techniques for rotational motion in two dimensions: quenched annealed and no-spin quantum statistical averages. Phys Rev A 1992; 45:8968–71.
[13] Wang QY, Johnson JK. Molecular simulation of hydrogen adsorption in single-walled carbon nanotubes and idealized carbon slit pores. J Chem Phys 1999;110:577–86.
[14] Marx D, Optiz O, Nielaba P, Binder K. Quantum effects on herringbone ordering of N_2 on graphite. Phys Rev Lett 1993; 70:2908–11.
[15] Gu C, Gao GH, Yu YX, Mao ZQ. Simulation study in single-walled carbon nanotubes. Int J Hydrogen Energy 2001;16:691–6.
[16] Darkrim FL, Levesque D. High adsorptive property of opened carbon nanotubes at 77 K. J Phys Chem B 2000;104: 6773–6.
[17] Dillon AC, Jones KM, Bekkedahl TA, Heben MJ, Kiang CH, Bethune DS, et al. Storage of hydrogen in single-walled carbon nanotubes. Nature 1997;386:377–9.
[18] Ye Y, Ahn CC, Witham C, Fultz B, Liu J, Rinzler AG, et al. Hydrogen adsorption and cohesive energy of single-walled carbon nanotubes. Appl Phys Lett 1999;74:2307–9.
[19] Liu C, Fan YY, Liu M, Cong HT, Cheng HM, Dresselhaus MS. Hydrogen storage in single-walled carbon nanotubes at room temperature. Science 1999;286:1127–9.
[20] Zhu HW, Ci LJ, Chen A, Mao ZQ, Xu CL, Xiao X, et al. Hydrogen energy progress XIII, In: proceedings of the 13th World hydrogen energy conference. International association for hydrogen energy. Beijing (China); 2000. p. 560–64.
[21] Wu HB, Chen P, Lin J, Tan KL. Hydrogen uptake by carbon nanotubes. Int J Hydrogen Energy 2000;25:261–5.
[22] Basca R, Laurent C, Peigney A, Basca W, Vaugien T, Rousset A. High specific surface carbon nanotubes from catalytic chemical vapor deposition process. Chem Phys Lett 2000;323:566–71.
[23] Raffa V, Ciofani G, Nitodas S, Karachalios T, D'Alessandro D, Masini M, et al. Can the properties of carbon nanotubes influence their internalization by living cells? Carbon 2008; 46:1600–10.
[24] Nitodas S, Karachalios T. Low-cost production and applications of high purity carbon nanotubes. To be published in the international journal of nanomanufacturing (ijnm)-special issue of ISNM-06; 2008.
[25] Kouravelou KB, Sotirchos SV, Verykios XE. Catalytic effects of production of carbon nanotubes in a thermo-gravimetric CVD reactor. Surf Coating Tech 2007;201:9226–31.
[26] Kotsifa A, Kondarides DI, Verykios XE. Comparative study of the chemisorptive and catalytic properties of supported Pt catalysts related to the selective catalytic reduction of NO by propylene. Appl Catal B 2007;72:136.